



Adsorption of As(V) on zirconium-based adsorbents

Snigdha Khuntia, Subrata Kumar Majumder, Pallab Ghosh*

Department of Chemical Engineering, Indian Institute of Technology Guwahati, Guwahati 781039, Assam, India, email: snigdha@iitg.ernet.in (S. Khuntia), Tel. +91 361 2582265; Fax: +91 361 2582291; email: skmaju@iitg.ernet.in (S.K. Majumder), Tel. +91 361 2582253; Fax: +91 361 2582291; email: pallabg@iitg.ernet.in (P. Ghosh)

Received 1 February 2014; Accepted 10 October 2014

ABSTRACT

Adsorption of As(V) on zirconium impregnated activated carbon and amorphous zirconium oxide has been reported in this work. The adsorption of As(V) on both of these adsorbents was fast and effective. The As(V) adsorption capacity of amorphous zirconium oxide was larger than that of zirconium-activated carbon. Characterization of these adsorbents was performed by various methods (viz. SEM, EDX, XRD, and FTIR). The electric charge on the surface of these adsorbents in aqueous media was measured at different pH. The adsorption of As(V) followed a pseudo-second-order kinetics. However, from the intra-particle diffusion model, it was found that film-diffusion and intra-particle diffusion took place simultaneously during adsorption. Langmuir, Freundlich, and Redlich–Peterson adsorption isotherms were fitted to the experimental data. The adsorption of As(V) on these adsorbents was found to be spontaneous and endothermic in nature. The thermodynamic parameters (viz. changes in Gibbs free energy, enthalpy, and entropy) were calculated at different temperatures.

Keywords: Activated carbon; Adsorption; Arsenic; Isotherm; Zirconium

1. Introduction

Contamination of ground water due to arsenic is one of the crucial problems in many countries. Arsenic causes various adverse effects on human health, which have been extensively reported in the literature [1–5]. Arsenic exists in four oxidation states, viz. -3 (arsenide), 0 (elemental or metallic arsenic), $+3$ (arsenite), and $+5$ (arsenate). The -3 and 0 oxidation states of arsenic are rare in the environment [6]. Pentavalent arsenic [i.e. As(V) or arsenate] and trivalent arsenic [i.e. As(III) or arsenite] are commonly found in surface and ground waters as well as in soils and sediments. Although the World Health Organization (WHO) has

suggested a provisional upper limit of 0.01 mg/L arsenic in drinking water [7], the acceptable upper limit of arsenic in different countries varies significantly (e.g. 0.01 mg/L in India and 0.05 mg/L in Bangladesh) [8,9].

The speciation of arsenic in water and soil changes depending on the redox potential and the pH of the subsurface environment [7]. The oxidation of different mineral species present in soil is another controlling factor, which allows arsenic to become soluble and enter into the surrounding environment through water [10]. The most commonly used arsenic removal techniques are anion exchange, adsorption, reverse osmosis, coagulation/filtration, lime softening, and oxidation/filtration. Oxidation of As(III) to As(V)

*Corresponding author.

followed by the removal of the latter is a suitable technology for removal of arsenic from water [10–13]. Many chemical oxidants have been used for this oxidation such as chlorine dioxide, sodium hypochlorite, monochloroamine, potassium permanganate [14–16], manganese oxide [17–19], potassium ferrate [20], hydrogen peroxide [21], and ozone [22]. The dominant non-ionic species of As(III), viz. H_3AsO_3 , is not as strongly adsorbed on mineral surfaces as As(V) up to pH 8. Therefore, the pre-oxidation of As(III) to As(V) leads to a higher removal efficiency of arsenic by many adsorbents [7,20]. Of late, many biological materials, mineral oxides, activated carbons, polymeric resins, and other low cost adsorbents have been developed, which are very effective in removing As(V) [7,10,22]. Several types of activated carbons have been prepared and studied for removal of arsenic from wastewater [23–25]. However, activated carbons impregnated with a metal (e.g. iron, zirconium, copper, and silver) are more promising for arsenic removal as compared to untreated activated carbon [23,26,27]. Several works have reported adsorption of As(III) and As(V) on zirconium-loaded resins [28–30], zirconium-loaded activated carbons [26,31], and zirconium nanoparticles [32]. However, the methods of preparation of these resins and activated carbons are not very easy, whereas the nanoparticles are difficult to settle and remove.

The aim of this work is to prepare two potential zirconium-based adsorbents (i.e. zirconium-activated carbon and amorphous zirconium oxide) for As(V) adsorption using simple preparation methods. This study comprises synthesis and characterization of the adsorbents, determination of charge on their surface in aqueous solutions of different pH, development of adsorption isotherms, and evaluation of kinetic and thermodynamic parameters. The experimental data are enunciated by Langmuir, Freundlich, and Redlich–Peterson adsorption isotherms. Changes in Gibbs free energy, enthalpy, and entropy during adsorption are also calculated at different temperatures.

2. Materials and methods

2.1. Reagents

Arsenic (III) oxide (99.5% assay), zirconium oxychloride octahydrate ($\text{ZrOCl}_2 \cdot 8\text{H}_2\text{O}$, 98.5% assay), and activated charcoal were purchased from Loba Chemie (India). Arsenic (V) oxide (99.9% assay) and zirconium dinitrate oxide hydrate ($\text{ZrO}(\text{NO}_3)_2 \cdot 8\text{H}_2\text{O}$, 99.9% assay) were purchased from Alfa Aesar (India). Standard solution of arsenic (995 ± 5 mg/L), potassium iodide (99.8% assay), hydrochloric acid (35% assay),

potassium bromide (99.9%), and ammonia solution (30% assay) were purchased from Merck (India). Sodium hydroxide (>98% assay) was purchased from Rankem (India), and sodium borohydride (96% assay) was purchased from Spectrochem (India). Aqueous solutions required for the analysis were prepared using water that was purified by a Millipore water purification system (Millipore, USA, model: Elix-3).

2.2. Methods

2.2.1. Measurement of arsenic concentration

The concentration of arsenic was measured using an atomic absorption spectrophotometer (Varian, the Netherlands, model: Spectra AA 220FS) equipped with vapor generation assembly (which operated at 1,198 K) [33]. The sample was acidified using 7 M HCl. The generation of hydride was achieved by a continuous-flow mixing of the acidified sample using potassium iodide and sodium borohydride (viz. 0.6% NaBH_4 dissolved in 0.5% NaOH).

2.2.2. Preparation of adsorbents

Activated carbon was impregnated with zirconium by the method given by Okumura et al. [34]. Aqueous zirconyl nitrate solution (5.9%) was prepared by dissolving zirconyl nitrate dihydrate in water. The activated carbon was crushed and sieved to prepare 200 μm size, washed with deionized water several times, and dried in an oven at 398 K for 24 h. The purified activated carbon (50 g) was mechanically mixed with 500 mL of zirconyl nitrate solution for 3 d at 398 K. After that, the adsorbent was filtered and washed to purge the excess zirconyl nitrate. The filtered adsorbent was dried at 323 K for 48 h.

The amorphous zirconium oxide particles were prepared by the method described by Cui et al. [35]. Zirconium oxychloride solution (0.035 M) was prepared by dissolving zirconium octahydrate in water. The solution was magnetically stirred for 5 min. Thereafter, 50 mL of aqueous ammonia solution was slowly added to 20 mL of zirconium oxychloride solution with rigorous stirring. The stirring was continued for 5 min. The amorphous zirconium oxide precipitate was then dried in a hot air oven for 4 h at 423 K. The precipitate was subsequently cooled at room temperature, thoroughly washed with water to remove chloride, and then dried in the oven for 8 h at 383 K. It was then crushed to the desired size. The average diameter of the particles was ~ 50 μm . The particle size was determined by a laser particle size analyzer (Malvern, UK, model: Mastersizer 2000).

2.2.3. Characterization of adsorbents

The scanning electron microscope (SEM) (Leo, England, model: 1430vp) was used to image the surface of the adsorbents. The chemical composition of zirconium-activated carbon was analyzed using energy dispersive X-ray microanalyzer (EDX) (Oxford instruments, England, model: 7353), which was connected with the SEM. The crystal structure of the adsorbents was analyzed by a X-ray diffractometer (XRD) (Bruker, Germany, model: D8 Advance) at a step size of 0.1 s^{-1} .

Fourier transform infrared spectroscopy (FTIR) was used to analyze the functional groups of the adsorbents. A FTIR spectrophotometer (Shimadzu, Japan, model: IRAffinity-1) was used for this purpose. Dried adsorbents were ground with KBr in a fixed weight ratio (viz. sample : KBr = 1:100). All infrared spectra were generated at room temperature in transmission mode.

Zeta potential on the surface of the adsorbents was measured by the electrophoretic mobility of the fine particles of the adsorbents in a zeta potentiometer (Beckman Coulter, Switzerland, model: Delsa Nano). The procedure was similar to that reported in the literature [36,37]. The pH was adjusted in the range 1–12 using 0.1 M NaOH and 0.1 M HCl. It was measured by a pH meter (Eutech, Singapore, model: pH 2,700). 0.1 g of adsorbent was dispersed in 50 mL of water and shaken for 12 h. The zeta potential at the surface of the dispersed adsorbent particles was measured thereafter. No additional electrolyte was added, and the absolute values of zeta potential of the adsorbents are reported.

A BET surface analyzer (Beckman Coulter, Switzerland, model: SA 3100) was used to measure the surface area and pore volume of the adsorbents. The samples were degassed using helium at 473 K for 2 h. The surface area was obtained from the nitrogen adsorption isotherms.

2.2.4. Batch adsorption studies of As(III) and As(V)

All batch experiments on adsorption of As(III) and As(V) were carried out in 250 mL Erlenmeyer flasks at different temperatures. The working volume of the heterogeneous mixture was 200 mL and the adsorbent/adsorbate ratio was 1 g/L. Stock solutions of 100 mg/L arsenic trioxide and arsenic pentoxide were prepared by dissolving the respective compounds in water at the required pH. The concentration of the solutions was varied by successive dilution of the stock solution. The initial As(V) concentrations were

25, 50 and 100 $\mu\text{g/L}$. The pH was maintained using 0.1 M NaOH and 0.1 M HCl.

Kinetics of adsorption was studied by taking different initial concentrations of As(V) (viz. 25, 50 and 100 $\mu\text{g/L}$) at a constant adsorbent dose (viz. 1 g/L). At a particular time interval, samples were withdrawn and filtered through Whatman filter paper No. 1 (particle retention: 11 μm), and the concentration of As(V) was measured. The adsorbent particles settled quickly. The size of the adsorbent particles was $>20\text{ }\mu\text{m}$.

100 mL of As(V) solutions (having concentration in the range of 0.05–5 mg/L) were kept in contact with 0.1 g of adsorbent for 24 h at 298 K, and were shaken at a speed of 200 rpm. The pH of the solution was 6. The equilibrium concentration of As(V) was measured after 24 h of contact time. The amount of arsenic adsorbed on the surface of the adsorbent was calculated as the difference between the initial and equilibrium concentrations.

To determine the thermodynamic parameters for the adsorption of As(V), 100 mL of 1 mg/L As(V) solution was contacted with 0.1 g of the adsorbent at temperatures in the range of 298–318 K at pH 6. The shaking speed was 200 rpm. The equilibrium concentration of As(V) was measured after 24 h of contact time.

3. Results and discussion

3.1. Characterization of the adsorbents

The SEM images of the activated carbon and zirconium-activated carbon before the adsorption of As(V) are shown in Fig. 1(a) and (b), respectively. It is observed from these micrographs that these adsorbents had different textures. The activated carbon surface had porous structure. However, after the zirconium impregnation, these pores were filled up with the zirconium nanoparticles (Fig. 1(b)). This made the adsorbent efficient in the water treatment process, as it can be used repeatedly without losing the zirconium nanoparticles from the pores of the activated carbon. The distribution of pores was not uniform along the surface. From the EDX spectra of the zirconium-activated carbon, it was observed that the surface of the activated carbon was loaded with 2.92 atomic% (viz. 18.61 wt.%) of zirconium (Fig. 1(c)). After the adsorption of As(V), the EDX spectra showed another peak for arsenic. Fig. 1(d) shows that the adsorption of As(V) on the zirconium-activated carbon was effective, and the impregnated zirconium nanoparticles did not come out after the adsorption was carried out. The XRD pattern of zirconium-activated carbon before and after As(V) adsorption

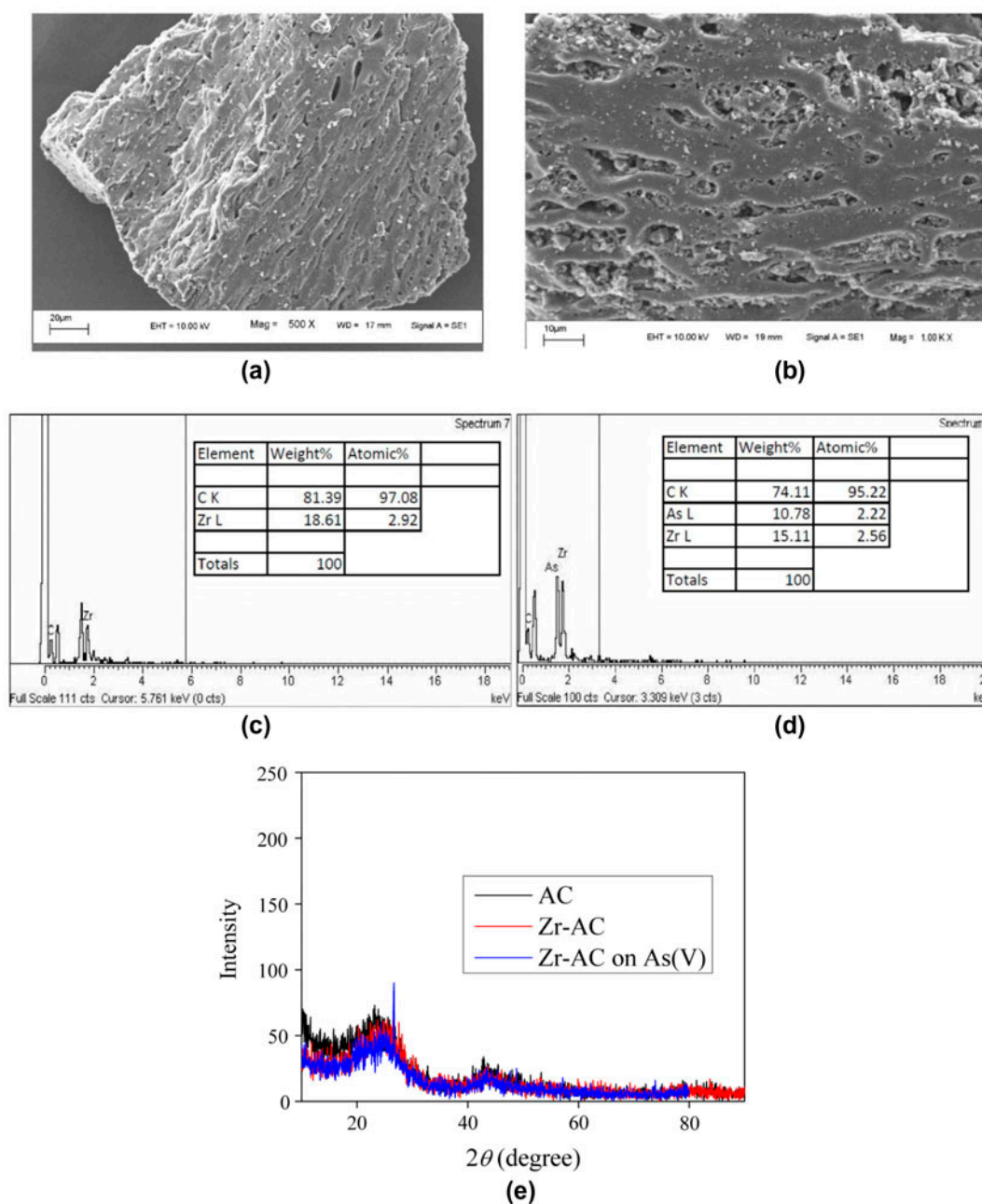


Fig. 1. SEM of (a) activated carbon and (b) zirconium-activated carbon (Zr-AC) before adsorption of As(V); (c) EDX of zirconium-activated carbon before adsorption of As(V) and (d) EDX of zirconium-activated carbon after adsorption of As(V); (e) XRD of zirconium-activated carbon before and after adsorption of As(V). θ (degree) represents the angle of diffraction.

shows the wide diffraction peak and weak peak intensity (Fig. 1(e)). This indicates that the zirconium-activated carbon was amorphous in nature. From the XRD pattern, it was observed that neither the impregnation of zirconium on activated carbon nor the adsorption of As(V) on it changed the morphology of these adsorbents.

The SEM image of zirconium oxide shows that the surface morphology of the adsorbent was amorphous and formed a tooth-like structure (Fig. 2(a)). The surface of the adsorbent was rough and porous. From the XRD pattern of amorphous zirconium oxide, two major diffraction peaks of the tetragonal ZrO_2 phase at $2\theta = 30^\circ$ and 50° were observed. However, the wide

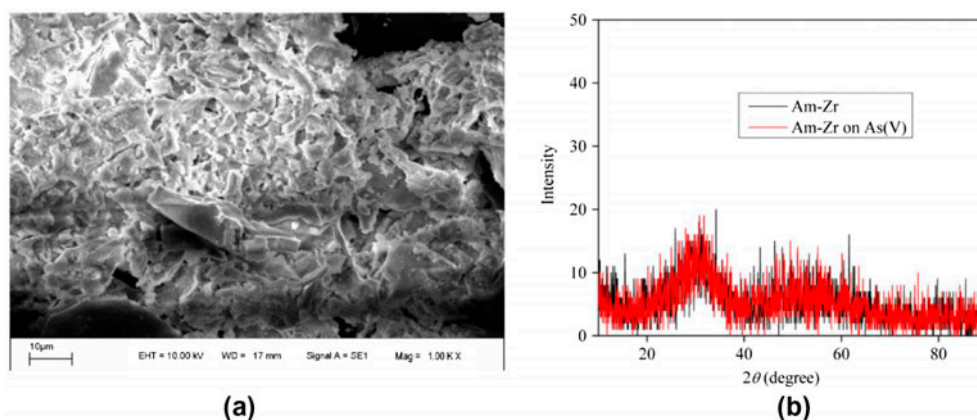


Fig. 2. (a) SEM of amorphous zirconium oxide (Am-Zr) and (b) XRD of amorphous zirconium oxide before and after adsorption of As(V).

diffraction peak and the weak peak intensity showed that the prepared zirconium oxide was amorphous in nature (Fig. 2(b)).

The specific surface area of the zirconium-activated carbon, determined from the BET surface area analyzer, was 737 m²/g. About 70.8% of total pores were in the range of 6–40 nm diameter, with the total pore volume of 0.45 mL/g. This indicates a very high mesopore volume. The specific surface area of the amorphous zirconium oxide was 478 m²/g. The amorphous zirconium oxide was highly mesoporous. About 86% of the pores had diameter in the range of 6–40 nm, and the total pore volume was 0.52 mL/g.

3.2. Effect of pH on adsorption of As(III) and As(V)

The adsorption profiles of As(V) on zirconium-activated carbon and amorphous zirconium oxide are shown in Fig. 3(a). It was observed that As(V) was adsorbed more on amorphous zirconium oxide at all As(V) concentrations. In order to determine the effective pH ranges for adsorption of As(III) and As(V), 50 µg/L of As(V) and 1 g/L of the adsorbent were stirred at 298 K at different pH. Fig. 3(b) illustrates the effect of pH on adsorption of As(III) and As(V). The untreated granular activated carbon shows a poor adsorption of both As(III) and As(V). The effective pH range for adsorption of As(III) on zirconium-activated carbon was found to be 5–8, and the same for As(V) was 4–9. For amorphous zirconium oxide, the effective adsorption of As(III) was observed at pH in the range of 3–8, and for As(V) the range was 3–9. However for both the adsorbents, it was observed that the adsorption of As(V) was more than that of As(III) at

pH in the range of 4–9. From these results, it can be concluded that zirconium-activated carbon and amorphous zirconium oxide can be used as suitable adsorbents for As(V) adsorption in the aforesaid range of pH.

The zeta potential is a measure of the electric potential at the surface of shear, which lies very close to the interface between water and the solid. The value of zeta potential was measured at different pH to determine the surface charge of the adsorbents and its role in the adsorption of As(V). The adsorption of As(III) and As(V) depends on the surface charge of the adsorbents as well as the speciation of arsenic at different pH. In aqueous solution, As(V) exhibits anionic behavior in the pH range of 2–11 [38]. The variation of zeta potential with pH is shown in Fig. 4. It is observed from this figure that the surface charge of the adsorbents was positive in acidic conditions, and it became negative in the alkaline media. The point of zero charge was observed at pH 5 for activated carbon, and the same was observed at higher values of pH for the other adsorbents. The adsorption of negatively charged As(V) species was stronger in the acidic condition, which has been depicted in Fig. 3(b). The value of zeta potential at the zirconium-activated carbon surface was positive at pH in the range of 1–8. This suggests that As(V) can be efficiently adsorbed at this pH range. At pH 8.5, the value of zeta potential was zero. The amorphous zirconium oxide surface showed positive charge at the acidic pH. The highest value of zeta potential was observed at about pH 4, and the magnitude of zeta potential was higher than that of the zirconium-activated carbon, for which the value of zeta potential was zero at pH 8.

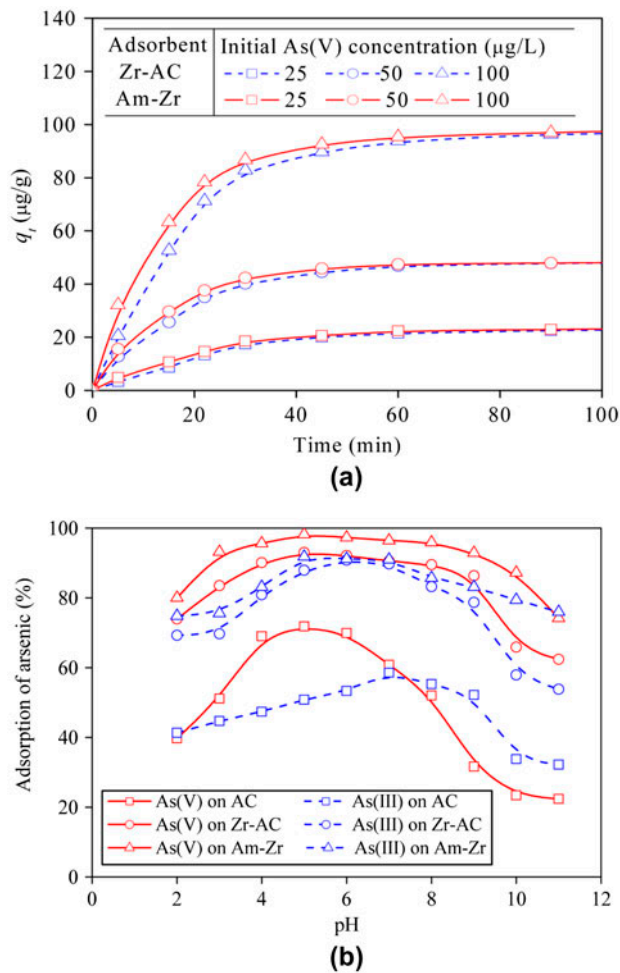


Fig. 3. (a) Adsorption profile of As(V) on amorphous zirconium oxide and zirconium-activated carbon and (b) Effect of pH on adsorption of As(III) and As(V) on activated carbon (AC), zirconium-activated carbon (Zr-AC), and amorphous zirconium oxide (Am-Zr). Initial arsenic concentration = 50 µg/L, shaking speed = 200 rpm, contact time = 3 h, temperature = 298 K, and adsorbent dose = 1 g/L.

3.3. Kinetics of adsorption

Three kinetic models (viz. pseudo-first-order, pseudo-second-order, and intra-particle diffusion) were used to study the adsorption of As(V) on zirconium-activated carbon and amorphous zirconium oxide. The main objective of this study was to determine the controlling mechanism of the adsorption process. The amount of As(V) adsorbed per unit mass of adsorbent q_t (µg/g) at time t (min) is given by:

$$q_t = (C_0 - C_t)V/M \quad (1)$$

where C_0 and C_t (µg/L) are the concentrations of As(V) at the beginning and after time t , respectively, V

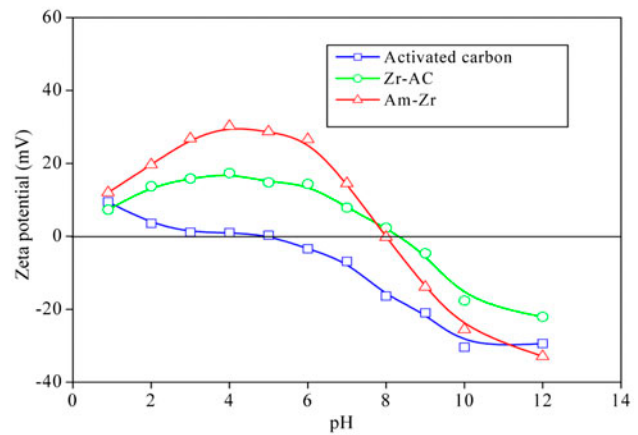


Fig. 4. The variation of zeta potential of activated carbon (AC), zirconium-activated carbon (Zr-AC), and amorphous zirconium oxide (Am-Zr) with the pH of the aqueous medium.

(L) is the volume of the solution, and M (g) is the mass of the adsorbent. It is observed that the time required to attain equilibrium depends on the initial adsorbate concentration. The adsorption was faster for a higher initial As(V) concentration, although the time required to attain the equilibrium was longer. For example, the time required to attain equilibrium was 1.5 h for 100 µg/L initial As(V) concentration, whereas the same for 25 µg/L initial As(V) concentration was 1 h.

According to the pseudo-first-order kinetic model, the rate of change of adsorbate uptake with time is directly proportional to the difference between the saturation concentration and the amount of adsorbate uptake up to that time. The first-order rate equation for adsorption is expressed as [39]:

$$dq_t/dt = k_1(q_e - q_t) \quad (2)$$

where q_e and q_t (µg/g) are the amounts of As(V) adsorbed at equilibrium and at time t , respectively. k_1 (min^{-1}) is the rate constant for adsorption. Integrating Eq. (2), we get:

$$\ln(q_e - q_t) = \ln(q_e) - k_1t \quad (3)$$

Eq. (3) suggests that the plot of $\ln(q_e - q_t)$ vs. t will be linear. This is shown in Fig. 5(a). The adsorption rate constant and the equilibrium adsorption capacity were calculated from the slope and intercept, respectively. These values are presented in Table 1. The coefficient of determination (ρ^2) for zirconium-activated carbon and amorphous zirconium oxide was found to be 0.94 and 0.98, respectively.

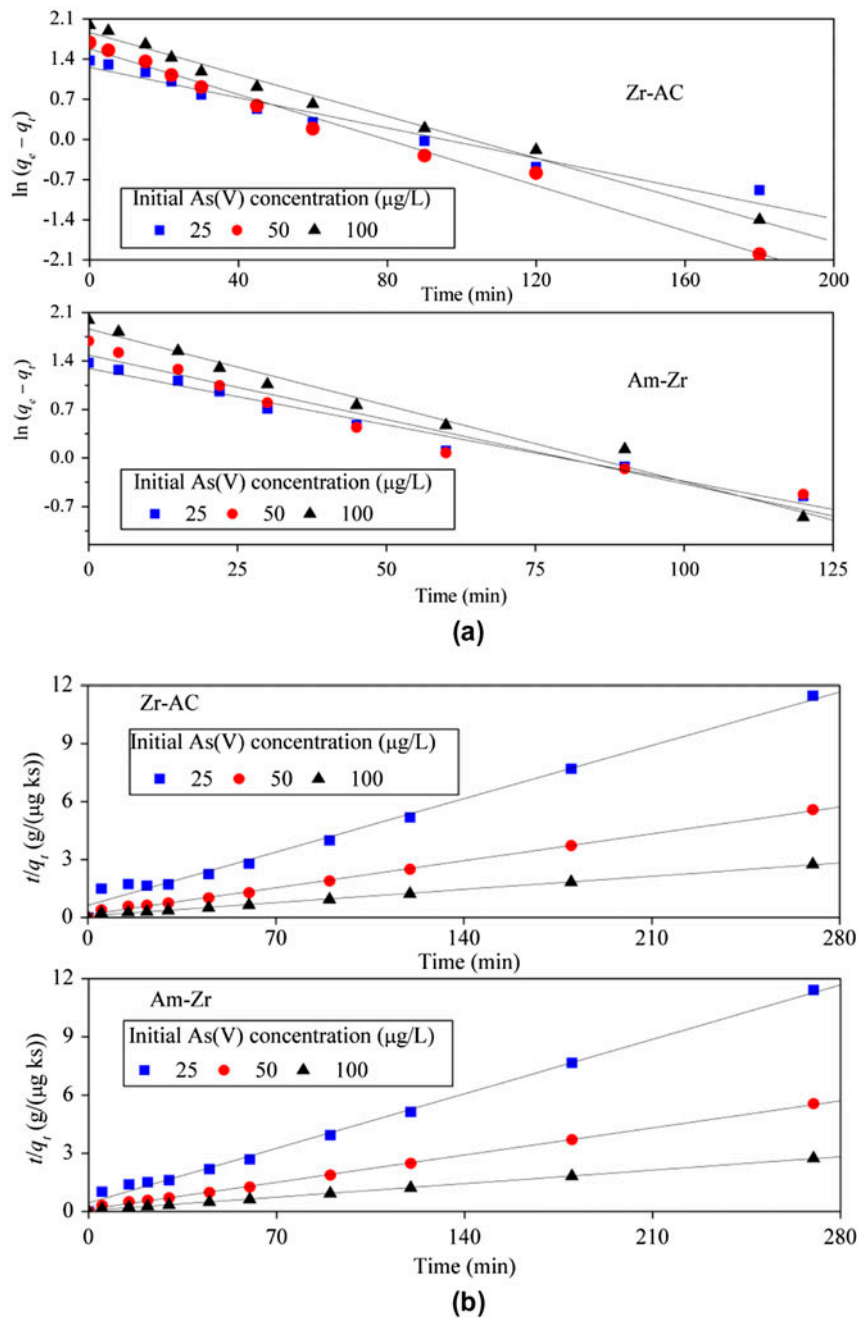


Fig. 5. (a) Pseudo-first-order kinetic model and (b) pseudo-second-order kinetic model for the adsorption of As(V) on the adsorbents (adsorbent dose = 1 g/L, temperature = 298 K, shaking speed = 200 rpm, and pH = 6 ± 0.2).

Although Eq. (3) fitted the experimental data reasonably well, the second-order model was explored to determine the best kinetic model to describe the mechanism of As(V) adsorption on these adsorbents. The equation for pseudo-second-order kinetic model is given by [39]:

$$\frac{t}{q_t} = \frac{1}{k_2 q_e^2} + \frac{t}{q_e} \quad (4)$$

where k_2 (g/(μg min)) is the pseudo-second-order rate constant. Eq. (4) suggests that a plot of t/q_t with t would be a straight line. From the slope and the

Table 1
Kinetic model parameters for adsorption of As(V) at 298 K

Kinetic model	Parameters $C_0(\mu\text{g/L})$	Zirconium-activated carbon			Amorphous zirconium oxide		
		25	50	100	25	50	100
Pseudo-first-order	$q_e^{\text{cal}} (\mu\text{g/g})$	17.9	37.7	72.6	19.6	30.4	72.8
	$q_e^{\text{expt}} (\mu\text{g/g})$	23.5	48.4	98.0	23.7	48.7	98.4
	$k_1 (\text{min}^{-1})$	0.013	0.019	0.018	0.016	0.018	0.022
	ρ^2	0.97	0.99	0.99	0.97	0.95	0.98
Pseudo-second-order	$q_e^{\text{cal}} (\mu\text{g/g})$	26.3	52.6	111.1	25.6	52.7	110.6
	$q_e^{\text{expt}} (\mu\text{g/g})$	23.5	48.4	98.0	23.7	48.7	98.4
	$k_2 \times 10^3 (\text{g}/(\mu\text{g min}))$	1.90	1.99	0.82	2.80	2.80	1.30
	ρ^2	0.99	0.99	0.99	0.99	0.99	0.99
Intra-particle diffusion	$k_i^1 (\mu\text{g}/(\text{g ks}^{0.5}))$	3.96	7.40	16.10	3.71	7.00	13.87
	$I_1 (\mu\text{g/g})$	5.60	2.34	10.52	3.18	2.05	6.90
	ρ^2	0.98	0.97	0.95	0.98	0.96	0.94
	$k_i^2 (\mu\text{g}/(\text{g ks}^{0.5}))$	0.31	0.32	0.71	0.25	0.24	0.52
	$I_2 (\mu\text{g/g})$	19.02	43.84	87.78	20.10	45.30	91.10
	ρ^2	0.97	0.95	0.94	0.97	0.97	0.95

intercept, the values of q_e and k_2 can be determined. These plots are shown in Fig. 5(b). The values of q_e and k_2 are presented in Table 1. The coefficient of determination for both the adsorbents was ~ 0.99 for all As(V) concentrations. According to the intra-particle diffusion model, q_t varies with t as [40]:

$$q_t = k_i \sqrt{t} + I \quad (5)$$

where k_i ($\mu\text{g}/(\text{g min}^{0.5})$) is the intra-particle diffusion rate constant and I ($\mu\text{g/g}$) is the intercept. As per this model, the adsorption process takes place via four steps. The movement of adsorbate molecules from bulk solution to the surface of the adsorbent by bulk diffusion occurs in the first step. In the second step, diffusion of adsorbate molecules takes place through the boundary layer to the surface of the adsorbent via film diffusion. In the third step, transport of the adsorbate molecules occurs from the surface to the interior pores of the particle by intra-particle or pore diffusion. In the final step, adsorption takes place at an active site on the surface of the material via ion exchange, complexation, and/or chelation.

Fig. 6 depicts the variation of q_t with time. The experimental data clearly depict two linear segments in as many time zones. Therefore, two steps are involved in the adsorption process. The initial sudden increase in the slope (i.e. the first linear segment) indicates that As(V) was transported to the external surface of the adsorbent through film diffusion and the rate was very fast. The second linear segment (at higher times) indicates a gradual adsorption, where

intra-particle diffusion was the rate-limiting step. Both the lines do not pass through the origin, which means both film and intra-particle diffusion took place simultaneously during the adsorption of As(V) on these adsorbents. The values of k_i^1 , k_i^2 , I_1 , I_2 , and ρ^2 are given in Table 1.

3.4. Adsorption isotherms

Three adsorption isotherms (viz. Langmuir, Freundlich, and Redlich–Peterson) were used for studying the adsorption of As(V). The Langmuir isotherm is given by [40]:

$$\frac{q_e}{q_{\text{max}}} = \frac{K_L C_e}{1 + K_L C_e} \quad (6)$$

where q_{max} (mg/g) is the maximum adsorption capacity corresponding to a complete monolayer coverage on the surface. C_e (mg/L) is the concentration of adsorbate at equilibrium, and K_L (L/mg) is the Langmuir constant which corresponds to the adsorption energy. In Eq. (6), q_e is expressed in mg/g. A dimensionless separation factor, r , describes the adsorption efficiency. It is defined as:

$$r = \frac{1}{1 + K_L C_0} \quad (7)$$

The process is irreversible if $r = 0$, linear if $r = 1$, and unfavorable if $r > 1$. For a favorable adsorption, the value of r should lie between 0 and 1 [41].

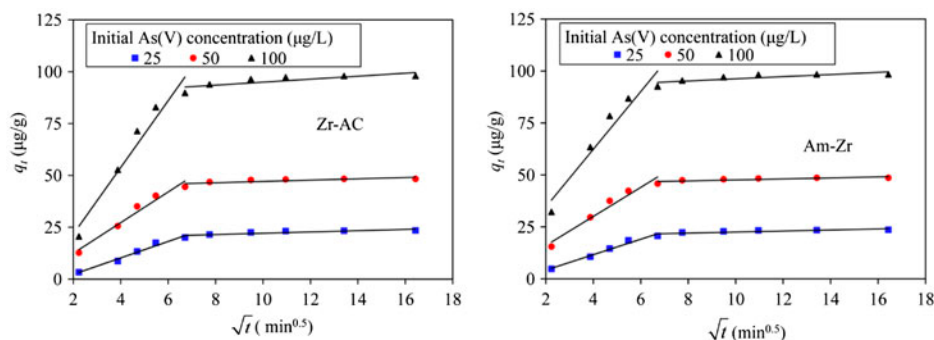


Fig. 6. Intra-particle diffusion model for adsorption of As(V) (adsorbent dose = 1 g/L, temperature = 298 K, shaking speed = 200 rpm, and pH = 6 ± 0.2).

According to the Freundlich adsorption isotherm, the adsorption energy decreases exponentially. This isotherm describes reversible adsorption and is not restricted to the formation of a monolayer. The Freundlich isotherm is given by [39]:

$$q_e = K_F C_e^n \quad (8)$$

where K_F ((mg/g) (L/mg) $^{1/n}$) is the Freundlich constant and n is the heterogeneity factor. K_F reflects the adsorption capacity. The value of n greater than unity indicates favorable adsorption conditions. Redlich and Peterson [42] incorporated three parameters into an empirical isotherm. This model combines elements from both the Langmuir and Freundlich equations, and the mechanism of adsorption is not restricted to the formation of a monolayer. The Redlich–Peterson isotherm is given by [42,43]:

$$q_e = \frac{AC_e}{1 + B(C_e)^g} \quad (9)$$

where A (L/g), B ((L/mg) g) and g are the Redlich–Peterson constants.

The constants of Langmuir isotherm were calculated by regression analysis. These values are presented in Table 2. The maximum adsorption capacity, q_{\max} , of the adsorbent increased with increasing temperature. This indicates that the adsorption of As(V) on zirconium-activated carbon and amorphous zirconium oxide was endothermic in nature. The value of K_L remained almost constant with increasing temperature from 298 to 308 K. However, it decreased at 318 K. The As(V) adsorption capacity of amorphous zirconium oxide was found to be more than that of zirconium-activated carbon at all temperatures. The values of r for different initial concentrations of As(V)

(i.e. C_0) were between 0 and 1 for both the adsorbents (viz. 0.26–0.98 for zirconium-activated carbon and 0.17–0.96 for amorphous zirconium oxide) in the temperature range of 298–308 K. These values indicate a favorable adsorption system, and show that the data obeyed the Langmuir isotherm. The Freundlich isotherm constants were calculated from the linear plot of $\ln q_e$ vs. $\ln C_e$. For both the adsorbents, Freundlich isotherm gave a better fit than the Langmuir isotherm at all temperatures. The value of K_F increased with increasing temperature, which indicates that the adsorption efficiency of As(V) on both the adsorbents increased with increasing temperature. The value of n was very close to unity, which represents favorable adsorption conditions. The Redlich–Peterson isotherm was found to fit the data in the best manner, as shown in Fig. 7. The constants of Redlich–Peterson isotherm were determined by nonlinear regression. These values are given in Table 2. The Redlich–Peterson constant, A , increased, whereas the value of the constant, B , decreased with increasing temperature. The exponent, g , in Redlich–Peterson isotherm was found to lie between 0 and 1.

From the adsorption isotherm studies, it was found that Langmuir, Freundlich, and Redlich–Peterson models fitted the data well for both the adsorbents. The monolayer adsorption capacity, q_{\max} , for these adsorbents was much higher than the zirconium-loaded activated carbon prepared by Daus et al. [26], close to the zirconium-based magnetic sorbent prepared by Zheng et al. [44], and zirconium resins [28,30]. However, Freundlich and Redlich–Peterson models fitted the data better than the Langmuir model. This indicates that multilayer adsorption of As(V) on zirconium-activated carbon and amorphous zirconium oxide took place via the surface functional groups [41].

Table 2

Langmuir, Freundlich, and Redlich–Peterson isotherm constants for adsorption of As(V) on zirconium-activated carbon and amorphous zirconium oxide

Isotherm	Parameters	Temperature (K)					
		Zirconium-activated carbon			Amorphous zirconium oxide		
		298	308	318	298	308	318
Langmuir	q_{\max} (mg/g)	42.60	47.60	58.80	50.30	55.60	66.70
	K_L (L/mg)	0.55	0.55	0.51	0.99	0.99	0.88
	ρ^2	0.98	0.98	0.99	0.96	0.96	0.97
Freundlich	K_F (mg/g)(L/mg) $^{1/n}$	19.30	21.50	25.90	40.90	45.70	49.90
	n	1.04	1.04	1.03	1.04	1.03	1.03
	ρ^2	0.99	0.99	0.99	0.99	0.99	0.99
Redlich–Peterson	A (L/g)	23.70	26.30	30.30	52.20	53.20	58.63
	B (L/mg) g	0.55	0.59	0.41	0.62	0.62	0.53
	g	1.00	0.96	0.93	0.62	1.00	0.78
	ρ^2	1.00	1.00	1.00	1.00	1.00	0.99

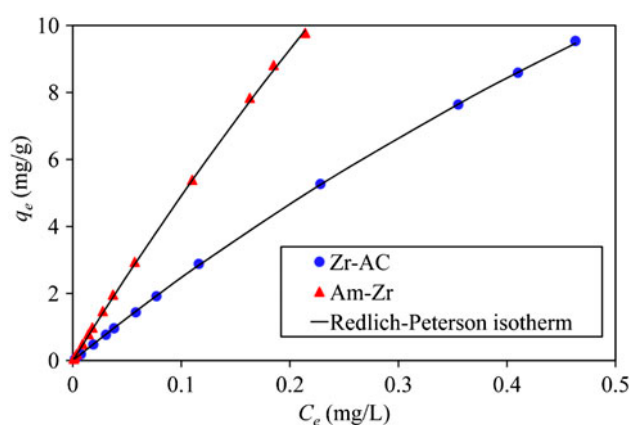


Fig. 7. The fit of Redlich–Peterson adsorption isotherm to the experimental data (at 298 K) for adsorption of As(V) on zirconium-activated carbon (Zr-AC) and amorphous zirconium oxide (Am-Zr).

3.5. Thermodynamic studies of As(V) adsorption

The changes in standard Gibbs free energy, ΔG^0 (kJ/mol), enthalpy, ΔH^0 (kJ/mol), and standard entropy, ΔS^0 (kJ/mol K), for the adsorption of As(V) were determined from Eqs. (10) and (11) as given below [41,44,45].

$$\ln K_c = \frac{\Delta G^0}{RT} = \frac{\Delta S^0}{R} - \frac{\Delta H^0}{RT} \quad (10)$$

where R is the gas constant (J/mol K) and T represents temperature (K). By plotting $\ln K_c$ against $1/T$, and fitting the data by a straight line, the values of ΔS^0 and ΔH^0 were determined from the intercept and

slope of the line, respectively. The value of ΔG^0 was calculated from the equation:

$$\Delta G^0 = -RT \ln K_c \quad (11)$$

where K_c is the distribution coefficient for adsorption. It is defined as the ratio, $q_e m / C_e$, where m is the concentration of adsorbent (g/L). The determination of ΔS^0 and ΔH^0 from the linear plots is shown in Fig. 8. The values of these thermodynamic parameters are given in Table 3. The positive values of ΔH^0 indicate that the adsorption of As(V) on both of these adsorbents was endothermic in nature. The value of heat of adsorption was found to be about 7.7–10.8 kJ/mol, which indicates that the adsorption was physical

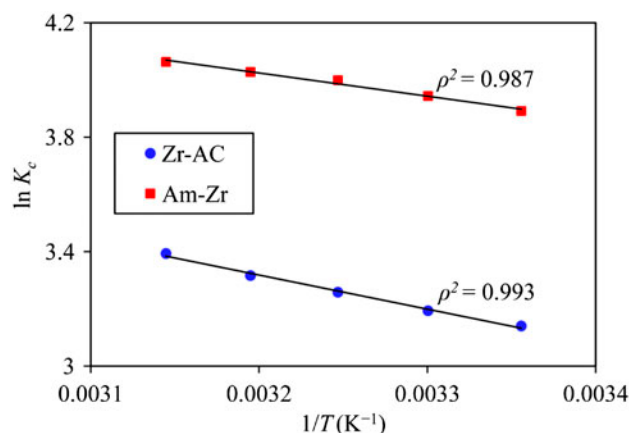


Fig. 8. Determination of ΔH^0 and ΔS^0 from the plot of $\ln K_c$ vs. $1/T$ for zirconium-activated carbon (Zr-AC) and amorphous zirconium oxide (Am-Zr).

Table 3

Thermodynamic parameters of adsorption of As(V) on zirconium-activated carbon and amorphous zirconium oxide

Adsorbent	Temperature (K)	ΔH^0 (kJ/mol)	ΔS^0 (kJ/mol K)	$-\Delta G^0$ (kJ/mol)
Zirconium-activated carbon	298	9.9	0.06	7.98
	303			8.28
	308			8.58
	413			8.88
	418			9.18
Amorphous zirconium oxide	298	6.7	0.06	11.18
	303			11.48
	308			11.78
	413			12.08
	418			12.38

rather than chemical [46]. The positive values of ΔS^0 indicate an increase in the randomness during adsorption. They reflect the affinity of the adsorbent for As(V). This is likely due to some structural changes in the arsenic species and the adsorbent [47]. Similar results have been reported in the literature [39,41,48,49]. The negative values of ΔG^0 indicate the spontaneity of the adsorption process.

3.6. FTIR studies of the adsorbents before and after As(V) adsorption

The mechanism of adsorption of As(V) on zirconium-activated carbon and amorphous zirconium oxide was investigated by FTIR spectroscopy. Fig. 9(a) shows the FTIR spectra of untreated activated carbon and zirconium-activated carbon before and after the adsorption of As(V). The hydroxyl stretching was found to be very poor for the untreated activated carbon (which is generally found at 3,100–3,700 cm^{-1}). However, zirconium-activated carbon showed a broad

region of hydroxyl functional group with a very prominent peak at 3,441 cm^{-1} , which is usually derived from the carboxylic and phenolic groups, and adsorbed H_2O molecules [50]. The small absorption bands at 2,924 and 2,850 cm^{-1} were due to the symmetric and asymmetric C–H stretching vibrations [50]. The peak at 1,589 cm^{-1} shows the vibrations of physically adsorbed H_2O [35]. The disappearance of the hydroxyl group (i.e. 3,441 cm^{-1}) after As(V) adsorption implies that the hydroxyl groups were involved in the adsorption of As(V). The broad bands appearing for activated carbon at 949 and 1,168 cm^{-1} are mainly related to the C–O stretching vibration of alcoholic, phenolic, and carboxylic groups. These bands disappeared after zirconium impregnation. This peak was replaced by the Zr–O bond and a strong peak appeared at 1,018 cm^{-1} . After adsorption of As(V), the peak at 1,018 cm^{-1} disappeared. This happened due to the formation of the As–OZr bond [35]. It was observed that the shape of the spectrum from 600 to 1,000 cm^{-1} of zirconium-activated carbon after As(V)

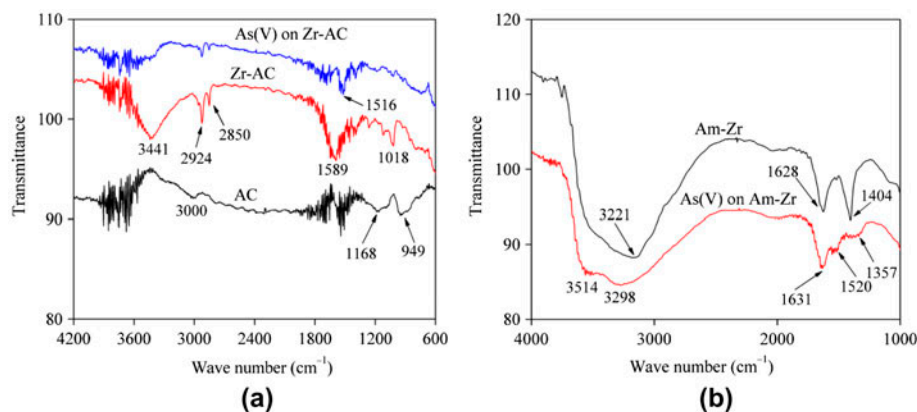


Fig. 9. FTIR spectra of (a) zirconium-activated carbon (Zr-AC) and (b) amorphous zirconium oxide (Am-Zr) before and after adsorption of As(V).

adsorption was different from that before adsorption. This change might be due to the formation of the complex of the arsenate ion with ZrO group [51].

Fig. 9(b) depicts the FTIR spectra of amorphous zirconium oxide before and after the adsorption of As(V). Before the adsorption of As(V), the FTIR spectra of amorphous zirconium oxide had a strong and prominent hydroxyl stretching at $3,221\text{ cm}^{-1}$. The peaks at $1,628$ and $1,404\text{ cm}^{-1}$ represent the adsorbed H_2O molecules and the Zr–OH group, respectively [35]. The broadening of the peak corresponding to the hydroxyl group after As(V) adsorption suggests the involvement of the hydroxyl group in the adsorption process. Furthermore, the peak at $1,404\text{ cm}^{-1}$ disappeared after adsorption and two smaller peaks at $1,357$ and $1,520\text{ cm}^{-1}$ appeared due to the formation of Zr–As bond by the replacement of the Zr–O bond.

4. Conclusion

Based on the experimental results and the analysis of the data, it was observed that As(V) strongly adsorbed on zirconium-activated carbon and amorphous zirconium oxide. Electric charge on the surface of these adsorbents changed from positive to negative as the pH of the aqueous medium was increased. The adsorption of As(V) was effective at slightly acidic conditions at which the value of the zeta potential was positive. The adsorbents were mesoporous with a large specific surface area. Both the adsorbents were amorphous in nature. The adsorption of As(V) followed pseudo-second-order kinetics. It also followed the intra-particle diffusion model. The adsorption isotherms were best fitted with the Freundlich and Redlich–Peterson models. The maximum adsorption capacity of amorphous zirconium oxide was greater than that of zirconium-activated carbon. The adsorption of As(V) on these adsorbents was spontaneous and endothermic in nature, and it led to an increase in the entropy.

Acknowledgment

The authors thank Department of Science and Technology (Water Technology Initiative), Government of India, for the financial support of this work, through the grant number: DST/TM/ WTI/2k10/266/(G), dated: September 5, 2011.

References

- [1] A. Juárez-Reyes, M.E. Jiménez-Capdeville, J.M. Delgado, D. Ortiz-Pérez, Time course of arsenic species in the brain and liver of mice after oral administration of arsenate, *Arch. Toxicol.* 83 (2009) 557–563.
- [2] S.B. Narahariseti, M. Aggarwal, S.N. Sarkar, J.K. Malik, Concurrent subacute exposure to arsenic through drinking water and malathion via diet in male rats: Effects on hepatic drug-metabolizing enzymes, *Arch. Toxicol.* 82 (2008) 543–551.
- [3] J.S. Petrick, F. Ayala-Fierro, W.R. Cullen, D.E. Carter, A.H. Vasken, Monomethylarsonous acid (MMAIII) is more toxic than arsenite in Chang human hepatocytes, *Toxicol. Appl. Pharmacol.* 163 (2000) 203–207.
- [4] C.K. Jain, I. Ali, Arsenic: Occurrence, toxicity and specification techniques, *Water Res.* 34 (2000) 4304–4312.
- [5] J.M. DeSesso, C.F. Jacobson, A.R. Scialli, C.H. Farr, J.F. Holson, An assessment of the developmental toxicity of inorganic arsenic, *Reprod. Toxicol.* 12 (1998) 385–433.
- [6] B.K. Mandal, K.T. Suzuki, Arsenic round the world: A review, *Talanta* 58 (2002) 201–235.
- [7] D. Mohan, C.U. Pittman Jr., Arsenic removal from water/wastewater using adsorbents – A critical review, *J. Hazard. Mater.* 142 (2007) 1–53.
- [8] M.M. Karim, Arsenic in groundwater and health problems in Bangladesh, *Water Res.* 34 (2000) 304–310.
- [9] D.G. Kinniburgh, P.L. Smedley, Arsenic contamination of groundwater in Bangladesh, Bangladesh department for public health engineering, British Geological Survey, Keyworth, Final report summary, 2000.
- [10] F.N. Robertson, Arsenic in ground-water under oxidizing conditions, south-west United States, *Environ. Geochem. Heal.* 11 (1989) 171–185.
- [11] S.K.R. Yadanaparthi, D. Graybill, R. von Wandruszka, Adsorbents for the removal of arsenic, cadmium, and lead from contaminated waters, *J. Hazard. Mater.* 171 (2009) 1–15.
- [12] C. Sullivan, M. Tyrer, C.R. Cheeseman, N.J.D. Graham, Disposal of water treatment wastes containing arsenic — A review, *Sci. Total Environ.* 408 (2010) 1770–1778.
- [13] L. Chen, H. Xin, Y. Fang, C. Zhang, F. Zhang, X. Cao, C. Zhang, X. Li, Application of metal oxide heterostructures in arsenic removal from contaminated water, *J. Nanomater.* 2014 (2014) 1–10.
- [14] G. Ghurye, D. Clifford, Laboratory study on the oxidation of arsenic III to arsenic V, EPA/600/R-01/021, Houston, TX, 2001.
- [15] G. Ghurye, D. Clifford, As (III) oxidation using chemical and solid-phase oxidants, *Am. Water Work. Assn.* 96 (2004) 84–96.
- [16] G. Lee, K. Song, J. Bae, Permanganate oxidation of arsenic(III): Reaction stoichiometry and the characterization of solid product, *Geochim. Cosmochim. Acta.* 75 (2011) 4713–4727.
- [17] W. Driehaus, R. Seith, M. Jekel, Oxidation of arsenate (III) with manganese oxides in water treatment, *Water Res.* 29 (1995) 297–305.
- [18] B.A. Manning, S.E. Fendorf, B. Bostick, D.L. Suarez, Arsenic(III) oxidation and arsenic(V) adsorption reactions on synthetic birnessite, *Environ. Sci. Technol.* 36 (2002) 976–981.
- [19] T. Nishimura, Y. Umetsu, Oxidative precipitation of arsenic(III) with manganese(II) and iron(II) in dilute acidic solution by ozone, *Hydrometallurgy* 62 (2001) 83–92.

- [20] M. Fan, R.C. Brown, C.P. Huang, Preliminary studies of the oxidation of arsenic(III) by potassium ferrate, *Int. J. Environ. Pollut.* 18 (2002) 91–96.
- [21] O.X. Leupin, S.J. Hug, Oxidation and removal of arsenic (III) from aerated groundwater by filtration through sand and zero-valent iron, *Water Res.* 39 (2005) 1729–1740.
- [22] S. Khuntia, S.K. Majumder, P. Ghosh, Oxidation of As (III) to As(V) using ozone microbubbles, *Chemosphere* 97 (2014) 120–124.
- [23] Z. Gu, J. Fang, B. Deng, Preparation and evaluation of GAC-based iron-containing adsorbents for arsenic removal, *Environ. Sci. Technol.* 39 (2005) 3833–3843.
- [24] C.L. Chuang, M. Fan, M. Xu, R.C. Brown, S. Sung, B. Saha, C.P. Huang, Adsorption of arsenic(V) by activated carbon prepared from oat hulls, *Chemosphere* 61 (2005) 478–483.
- [25] C.P. Huang, P.L.K. Fu, Treatment of arsenic(V)-containing water by the activated carbon process, *Water Pollut. Control Fed.* 56 (1984) 233–242.
- [26] B. Daus, R. Wennrich, H. Weiss, Sorption materials for arsenic removal from water: A comparative study, *Water Res.* 38 (2004) 2948–2954.
- [27] L.V. Rajakovic, The sorption of arsenic onto activated carbon impregnated with metallic silver and copper, *Sep. Sci. Technol.* 27 (1992) 1423–1433.
- [28] T.M. Suzuki, J.O. Bomani, H. Matsunaga, T. Yokoyama, Preparation of porous resin loaded with crystalline hydrous zirconium oxide and its application to the removal of arsenic, *React. Funct. Polym.* 43 (2000) 165–172.
- [29] X. Zhu, A. Jyo, Removal of arsenic(V) by zirconium (IV)-loaded phosphoric acid chelating resin, *Sep. Sci. Technol.* 36 (2001) 3175–3189.
- [30] T. Balaji, T. Yokoyama, H. Matsunaga, Adsorption and removal of As(V) and As(III) using Zr-loaded lysine diacetic acid chelating resin, *Chemosphere* 59 (2005) 1169–1174.
- [31] S. Peräniemi, S. Hannonen, H. Mustalahti, M. Ahlgrén, Zirconium-loaded activated charcoal as an adsorbent for arsenic, selenium and mercury, *Frese-nius J. Anal. Chem.* 349 (1994) 510–515.
- [32] R. Sandoval, A.M. Cooper, K. Aymar, A. Jain, K. Hristovski, Removal of arsenic and methylene blue from water by granular activated carbon media impregnated with zirconium dioxide nanoparticles, *J. Hazard. Mater.* 193 (2011) 296–303.
- [33] J.R. Behari, R. Prakash, Determination of total arsenic content in water by atomic absorption spectroscopy (AAS) using vapour generation assembly (VGA), *Chemosphere* 63 (2006) 17–21.
- [34] M. Okumura, K. Fujinaga, Y. Seike, K. Hayashi, A simple *in situ* preconcentration method for phosphate phosphorus in environmental waters by column solid phase extraction using activated carbon loaded with zirconium, *Anal. Sci.* 14 (1998) 417–419.
- [35] H. Cui, Q. Li, S. Gao, J.K. Shang, Strong adsorption of arsenic species by amorphous zirconium oxide nanoparticles, *J. Ind. Eng. Chem.* 18 (2012) 1418–1427.
- [36] A.L.P.F. Caroni, C.R.M. de Lima, M.R. Pereira, J.L.C. Fonseca, Tetracycline adsorption on chitosan: A mechanistic description based on mass uptake and zeta potential measurements, *Colloids Surf., B* 100 (2012) 222–228.
- [37] E.C.C. Gomes, A.F. de Sousa, P.H.M. Vasconcelos, D.Q. Melo, I.C.N. Diógenes, E.H.S. de Sousa, R.F. do Nascimento, R.A.S. San Gil, E. Longhinotti, Synthesis of bifunctional mesoporous silica spheres as potential adsorbent for ions in solution, *Chem. Eng. J.* 214 (2013) 27–33.
- [38] R. Ansari, M. Sadegh, Application of activated carbon for removal of arsenic ions from aqueous solutions, *E-Journal Chem.* 4 (2007) 103–108.
- [39] B.H. Hameed, A.A. Ahmad, N. Aziz, Isotherms, kinetics and thermodynamics of acid dye adsorption on activated palm ash, *Chem. Eng. J.* 133 (2007) 195–203.
- [40] B.K. Nandi, A. Goswami, M.K. Purkait, Adsorption characteristics of brilliant green dye on kaolin, *J. Hazard. Mater.* 161 (2009) 387–395.
- [41] A.Ö.A. Tuna, E. Özdemir, E.B. Şimşek, U. Beker, Removal of As(V) from aqueous solution by activated carbon-based hybrid adsorbents: Impact of experimental conditions, *Chem. Eng. J.* 223 (2013) 116–128.
- [42] O. Redlich, D.L. Peterson, A useful adsorption isotherm, *J. Phys. Chem.* 63 (1959) 1024–1024.
- [43] W. Shao, X. Li, Q. Cao, F. Luo, J. Li, Y. Du, Adsorption of arsenate and arsenite anions from aqueous medium by using metal(III)-loaded amberlite resins, *Hydrometallurgy* 91 (2008) 138–143.
- [44] T.S. Singh, K. Pant, Equilibrium, kinetics and thermodynamic studies for adsorption of As(III) on activated alumina, *Sep. Purif. Technol.* 36 (2004) 139–147.
- [45] L.A. Rodrigues, L.J. Maschio, R.E. da Silva, M.L.C.P. da Silva, Adsorption of Cr(VI) from aqueous solution by hydrous zirconium oxide, *J. Hazard. Mater.* 173 (2010) 630–636.
- [46] X. Du, Q. Yuan, Y. Li, Equilibrium, thermodynamics and breakthrough studies for adsorption of solanesol onto macroporous resins, *Chem. Eng. Process.* 47 (2008) 1420–1427.
- [47] L. Zeng, Arsenic adsorption from aqueous solutions on an Fe(III)-Si binary oxide adsorbent, *Water Qual. Res. J. Canada* 39 (2004) 267–275.
- [48] A. Goswami, P.K. Raul, M.K. Purkait, Arsenic adsorption using copper (II) oxide nanoparticles, *Chem. Eng. Res. Des.* 90 (2012) 1387–1396.
- [49] S. Mandal, T. Padhi, R.K. Patel, Studies on the removal of arsenic (III) from water by a novel hybrid material, *J. Hazard. Mater.* 192 (2011) 899–908.
- [50] G.Q. Wu, X. Sun, H. Hui, X. Zhang, J. Yan, Q.S. Zhang, Adsorption of 2,4-dichlorophenol from aqueous solution by activated carbon derived from moso bamboo processing waste, *Desalin. Water Treat.* 51 (2013) 4603–4612.
- [51] Y.M. Zheng, S.F. Lim, J.P. Chen, Preparation and characterization of zirconium-based magnetic sorbent for arsenate removal, *J. Colloid Interface Sci.* 338 (2009) 22–29.